Description and Overview of an Instrument Designed to Measure Line-of-Sight Delay Due to Water Vapor

G. M. Resch
Tracking Systems and Applications Section

M. C. Chavez and N. I. Yamane
Microwave Observational Systems Section

Eight dual-channel microwave radiometers have been constructed as a research and development effort for the Crustal Dynamics Project and the Deep Space Network. These instruments, known as water vapor radiometers, are primarily intended to demonstrate that the variable path delay imposed by atmospheric water vapor can be calibrated in microwave tracking and distance measuring systems but could also be used in other applications involving moist air meteorology and propagation studies. They are being deployed to various stations and observatories that participate in Very Long Baseline Interferometry (VLBI) experiments including the Deep Space Stations in Spain and Australia. In this paper we review the development history of these instruments, outline the theory of operation and overall design considerations, and sketch the instrumental parameters and performance characteristics.

I. Introduction

It takes longer for a radio wave to traverse an atmospheric path L relative to the time it would take to traverse the same path in a vacuum. The electrical path length L_e is just the integral of the refractive index of the atmosphere along the path. The difference ΔL between the electrical path length and the physical path length is simply,

$$\Delta L = 10^{-6}\int N\,ds \qquad (1)$$

where N is the refractivity at the point s along the path. The refractivity for the atmosphere as given by Smith and Weintraub (Ref. 1) is composed of two terms. The first and largest term is called the dry term and is proportional to the integrated dry air density. For most purposes it is sufficient to "weigh" the atmosphere at the zenith with a barometer in order to estimate the "dry" delay ΔL_d and then scale this zenith quantity to the line-of-sight using a cosecant elevation law. The second term contributing to the refractivity is a function of the atmospheric water vapor. The excess path delay in centimeters for this term of the refractivity is of the form,

$$\Delta L_v = 0.1723\int (\rho_v/T)\,ds \qquad (2)$$

where ρ_v is the vapor density in gm/m^3, T is the temperature in kelvin, and s is in meters. Unfortunately (for our applica-

tions) atmospheric water vapor is a highly variable and not well-mixed atmospheric constituent. As a result it is impossible to estimate the path delay in Eq. (2) with high accuracy from surface measurements alone.

In interferometric systems our primary observable is the differential time-of-arrival of a radio wave at the stations comprising the interferometer. In a ranging system the primary observable is the round-trip signal time. For both systems atmospheric water vapor along the signal path will impose an additional delay between 3 to 60 cm (one way) depending on how much vapor is in the atmosphere and the elevation angle of the observations. Typically, the baseline or range determination is derived from observations at several different elevation angles so that the mapping of propagation effect error into baseline or position is rather complex. In general, if one requires a system accuracy better than 10-12 cm then the vapor along the signal path must be measured. Of the several techniques that could be used to measure line-of-sight vapor delay, the most cost effective utilizes the techniques of passive remote sensing with a dual-channel microwave radiometer. The water vapor molecule emits spectral radiation at a frequency of 22.235 GHz, whose intensity is approximately proportional to the number of molecules (or the delay) along the line of sight. The presence of liquid water complicates the measurement problem as it contributes significantly to the intensity of the atmospheric emission but contributes very little to the excess path delay. However, with a second microwave channel it is possible to separate the vapor and liquid effects in all but the most severe weather situations.

II. History

At its inception, it was immediately recognized that the technique of Very Long Baseline Interferometry (VLBI) could be used to investigate a wide variety of geodetic and geophysical phenomena (e.g., see Ref. 2). The basic instrumentation appeared capable of centimeter-level measurement precision. Shapiro and Knight (Ref. 3) pointed out that the overall accuracy of VLBI would be limited by systematic effects. In particular, the variable delay imposed by tropospheric water vapor seemed to be the limiting error source.

In 1972 the Jet Propulsion Laboratory began a research task called ARIES (Astronomical Radio Interferometric Earth Surveying) under the leadership of P. F. MacDoran. The objective of this task was to demonstrate that VLBI could be used to study the deformation of the earth's crust. The idea was to use a transportable 9-m antenna as one end of an interferometer, with base stations at Goldstone and the Owens Valley Radio Observatory. If the transportable station was moved around a network of geophysically interesting sites in southern California it would be possible to compile a time history of three-dimensional baseline vectors whose changes in time would tell us something about the crustal deformation around major faults in this tectonically complex region. The accuracy goals for this task were beyond the capability of conventional surveying techniques. Our aim was to measure three-dimensional vector baselines up to 1000 km long with 3- to 5-cm accuracy in each component and 1- to 2-cm accuracy in length. Ong et al. (Ref. 4) demonstrated that the ARIES instrumentation was capable of 3-cm accuracy by measuring a 300-m baseline between the 9-m antenna and the 64-m antenna at Goldstone. Progress toward the reduction or elimination of other major error sources was underway. By 1974 it seemed that three-dimensional baseline accuracy of a few cm would be possible in just a few years — if only the water vapor problem could be solved.

During the summer of 1974 J. W. Waters and R. Longbothum compared a spacecraft prototype microwave radiometer with radiosondes launched at the El Monte Airport in an experiment to determine atmospheric delay using the techniques of passive remote sensing. Their regression analysis against radiosonde data indicated a level of agreement better than 2 cm (units of excess path delay). Later work by Winn et al. (Ref. 5) and Moran and Penfield (Ref. 6) extended this basic result. It was clear that this device, which became known as a water vapor radiometer (WVR) could be used to calibrate vapor-induced delay along the line of sight of a nearby antenna. If the water vapor delay along the line of sight at each station could be calibrated to 2 cm, then 3- to 5-cm VLBI system accuracy seemed possible. During this same period a VLBI data acquisition system was being developed at the Haystack Observatory that was well suited for the small mobile VLBI antennas that we intended to use in ARIES. It was clear that ARIES needed a WVR that would operate as an integral part of this much larger, fully automated VLBI data acquisition system. The WVR would have to operate unattended and require a minimum of operator attention. It must be well calibrated, stable, able to operate in all but the most severe weather conditions, and provide a vapor path correction that was accurate to better than 2 cm. There was also a need to understand the random and systematic error budget of the WVR and to develop an inversion algorithm to convert the WVR observable (brightness temperature) to path delay correction.

The technical aspects of demonstrating the performance of the WVR and specification of its system operation turned out to be the easy part of the problem. Finding the funding to actually build the kind of WVR that ARIES needed was a much more complicated, time consuming, and discouraging task. In late 1976, with the help of E. J. Johnston, ARIES was able to borrow the engineering model of a spacecraft radiometer and began a low key effort to modify and repackage the

device for VLBI support. In 1977, the VLBI group at Goddard Space Flight Center (GSFC) purchased two microwave receivers from Sense Systems Inc. (corresponding to the two channels of a WVR) with the intention of building their own WVR. Of course everyone realized that WVR calibration was needed on both ends of the interferometer. Both the ARIES and GSFC groups used the Owens Valley Radio Observatory (OVRO) as a base station and they simultaneously perceived a rare opportunity to act in their mutual self-interest and equip the observatory with a WVR. Support was obtained from the Caltech President's Fund to purchase one of the microwave receivers necessary to make a WVR, and GSFC purchased the second channel as well as two positioners. The ARIES group agreed to put all of these assorted pieces together to make three reasonably compatible WVRs. Our intention was to use these WVRs as tools to demonstrate the validity of the technique as it applies to VLBI support and then build units that were an optimum design for our application. In early 1978, with the support of the Goddard group, we received partial funding to package three WVRs. Several months later we received directions to construct two additional WVRs for the Crustal Dynamics Project (which was then coming into existence).

The situation in July 1978 was very chaotic. We had some of the parts for three WVRs, directions to put together five WVRs, no clear funding pattern, and were restricted from carrying over money from one fiscal year to the next. We decided that it would be less expensive and faster to construct the two additional WVRs "in house" and immediately began the purchase of long-lead-time parts. In the latter part of 1978 the Deep Space Network (Advanced Systems and Implementation Offices) added two more radiometers to what had now become a production line. A year later Project ARIES requested another WVR (its second unit). These units were given several numbers, R01, R02, $\cdots$, R08 according to the order in which we began work on the hardware. The "R" designation served to emphasize the R&D nature of the effort.

We were directed by JPL management to construct these WVRs in a manner that was consistent with the needs of both JPL and non-JPL users. This presented a problem in that we had already inherited the pieces of three radiometers and were constrained to use off-the-shelf components for the new units. Our approach to this problem was dictated by our stated goal – to build research tools that were capable of demonstrating that vapor delay could be calibrated in VLBI measurements. We did *not* attempt research in radiometer construction, but instead decided to adopt the "safe" design of a Dicke switched instrument taken largely from a spacecraft design. It was decided to standardize on the two frequencies 20.7 and 31.4 GHz, use doubly stabilized Dicke radiometers, and discard the cold load calibration in the Sense Systems receivers. The latter point was dictated by three factors: (1) the load was inaccurate, (2) it was operationally cumbersome to keep filled with liquid nitrogen, and (3) it presented severe packaging problems.

For three reasons we decided to mount the WVRs on their own positioner. First, we assumed that if the WVR would be used for any application other than VLBI support it should not tie up the VLBI antenna. Second, the procedure that we use to establish and check the temperature scale calibration (i.e., the tipping curve) is rather awkward and time consuming when performed on a large antenna. Third, preliminary analysis suggested that the only difference between the broad beam WVR and the smaller beam radio telescope would be in the short-period fluctuations of water vapor. Since most VLBI observations are the result of incoherently averaging up to 15 minutes of data, it effectively smoothes the fast but small vapor fluctuations. In order to simplify the interfacing we added a microcomputer controller to which the user can send simple commands and have the WVR point, take data, etc.

There were several minor areas of design, assembly, and/or construction in the first three instruments that we felt could be improved. The changes that were finally incorporated into units R04-R08 were dictated by the requirement that all WVRs appear identical to the user at the controller interface. Unfortunately it proved to be impractical to remove all of the differences between the different units. The most obvious remaining difference is that the vapor frequency of WVR-R02 and R03 is centered at 21 GHz (as compared to 20.7 GHz for all other units) and the slew rate is approximately a factor of 4 slower than the other radiometers. Thus the eight radiometers that have been deployed consist of three different microwave packages, two different positioners, and three slightly different microcomputer controllers. However, thanks to the software that resides in the microcomputer these differences are largely transparent to the user. The current plan is to mount units R01 and R07 on the edge of the antenna they are intended to calibrate and to use the fast mounts from these units to retrofit units R02 and R03.

In July 1979 the unit designated WVR-R03 was delivered to the Haystack Observatory. According to our original agreement with GSFC (which now managed the Crustal Dynamics Project), the WVRs would be merely bench tested at JPL. Each observatory would be responsible for engineering tests and calibration of the WVR it received. This arrangement was found to be impractical, so in late 1979 at the request of the Crustal Dynamics Project we agreed to test and calibrate each WVR prior to shipment. In addition, we would assist with installation of the WVR at those observatories that needed help, keep a stock of spare parts, assist with maintenance problems, provide a minimal level of documentation (i.e.,

consistent with R&D instruments), and provide the algorithm necessary to convert WVR output into a delay correction. In order to provide a backup capability for vapor calibration as well as a check on WVR operation, we also agreed to construct, test and calibrate a solar hygrometer to go along with each WVR. These extensions of our responsibilities turned out to be more difficult and time consuming than was originally anticipated. WVR-R02 was installed at OVRO in September 1980; unit R05 was installed at the Haystack Observatory in January 1981; unit R06 was installed on the ARIES electronics van (Mobile Van-2) also in January; unit R04 was installed at DSS 13 in February; unit R01 was delivered to ARIES (Mobile Van-1) in May; and unit R08 was installed at Ft. Davis in June 1981. As per our agreement with the Crustal Dynamics Project, we have purchased a modest stock of spare parts, some of which have been used to solve problems at several installations. We have installed the WVRs where it was necessary.

This paper is the first of a series that will constitute the "minimal" level of documentation. In later articles we will discuss the control module, the microwave package, the positioner, testing and calibration, the algorithms, and the solar hygrometers.

III. Remote Sensing of Water Vapor

The physics of atmospheric water vapor and the techniques used to sense it are well developed in Refs. 7 and 8. We shall merely summarize a few pertinent points in this paper. In Fig. 1 we see the apparent brightness temperature of the zenith atmosphere in the frequency interval 10 to 40 Ghz. The lower curve illustrates the behavior of the brightness temperature in the complete absence of atmospheric water vapor. The middle curve in Fig. 1 is drawn for the case of 2 gm-cm^{-2} of precipitable water vapor M_v, and the upper curve represents the spectrum for an additional 0.1 gm-cm^2 of liquid M_L that is assumed to exist as small droplets. This is a columnar measure; that is, if we were to take a column 1 cm^2 at the base that extended through the entire atmosphere and precipitated all of the vapor, we would wind up with 2 grams of water. For our application a "handy dandy" relationship to remember is:

$$\Delta L_v \simeq 6.3\, M_v \tag{3}$$

or, the excess path delay ΔL_v (in cm) is about 6 times the precipitable vapor content M_v (expressed in gm/cm^2). Thus the middle curve of Fig. 1 refers to a zenith vapor delay of 12.6 cm, representing roughly average conditions over much of the United States. The reader should note that in the literature, precipitable vapor is often measured in centimeters (instead of gm/cm^2). This results in some confusion when instruments that measure precipitable vapor are compared with instruments that measure path delay.

The bump in the brightness temperature curve of Fig. 1 at the frequency of 22.235 GHz is due to an emission line from the water vapor molecule. If there is not a lot of water vapor along the line of sight (i.e., the line is not saturated), then the brightness temperature is roughly proportional to the columnar density plus the background radiation. The background radiation is due to three sources: (1) the blackbody radiation of the cosmos, which is known to be 2.9 K, (2) emission from the lower wings of higher frequency lines, in particular the band of oxygen lines near 60 GHz, and (3) emission and scattering of radiation from liquid water droplets that occur in clouds or rain. The emission from oxygen is calculable and can be removed from the observations. The presence of liquid water has little effect on the path delay but considerable effect on the brightness temperature, thereby confusing the vapor measurement. With measurements at two frequencies we can separate the vapor and liquid contributions.

If the average diameter of the water droplets is small compared to observing wavelength, then the spectrum of the radiation from the liquid component will vary as frequency squared (Ref. 9). At some frequency f_1 (near the vapor emission line) the brightness temperature T_{b1} will be proportional to $k_1\ \Delta L_v + k_2 M_L$, where k_1 and k_2 are constants, and M_L is the integrated liquid content. At some frequency f_2 (off the vapor emission line) the brightness temperature T_{b2}, will be proportional to $k_1'\ \Delta L_v + k_2' M_L$. If we observe these two brightness temperatures T_{b1} and T_{b2}, then we have two equations in two unknowns. Given the frequency-squared dependence of the liquid emission, these equations can be solved simultaneously for ΔL_v and M_L. We find that both the path delay and the precipitable liquid can be expressed as a linear combination of the observed brightness temperatures,

$$\Delta L_v \simeq a_0 + a_1 T_{b1} + a_2 T_{b2} \tag{4}$$

where a_0, a_1, and a_2 are "constants." This equation summarizes the basic measurement approach and is useful in considerations of performance of the measurement system. In actual use where observations are made at low elevation angles and in cloudy conditions, Eq. (4) is not a good approximation. A slightly more complicated expression analogous to the approach used in Ref. 10 will be derived in a later paper.

IV. The Instrumentation

A water vapor radiometer is simply a device for measuring sky brightness temperature at two frequencies on and near the

emission line at 22.2 GHz. It consists of two independent Dicke radiometers (see Ref. 11 for an explanation of the operation of a Dicke radiometer), one tuned to 20.7 GHz and the other tuned to 31.4 GHz. The RF electronics, switching circuitry, and power supplies comprise the microwave package. The microwave package is mounted atop a positioner that can point in azimuth and elevation. Both the microwave electronics and positioner are interfaced to the controller package that consists of a microcomputer and local control panel from which one can monitor any of the analog signals from either the microwave electronics or the positioner. The ability to monitor and control all WVR functions from the local control panel is very useful for diagnostic purposes. Under normal operating conditions, the microcomputer controls and acquires data from the microwave package and the positioner. The microcomputer can be interfaced to another computer (i.e., a host computer) or to a terminal via an RS-232 serial interface. A set of simple instructions is available to command the microcomputer to point the WVR, switch to internal loads, take data, etc. Figure 2 shows all three WVR modules; Figure 3 is a block diagram of the complete WVR.

V. System Requirements

In VLBI the basic observable is a group delay (Ref. 12), i.e., the differential time of arrival of a radio wave at the stations comprising the interferometer. Differing amounts of atmospheric water vapor surrounding the stations cause the observed group delay to differ from the calculated group delay (e.g., calculated from the geometry). Of course there are many other sources of error that lead to differences between observed and calculated delay. Our ability to either calibrate or "solve-for" these error sources sets the limit on the accuracy of the VLBI technique to measure vector distance. As discussed in Ref. 13, the analysis of VLBI error sources suggests that baseline accuracies of 3 to 5 cm are possible if the line-of-sight water vapor effects can be calibrated to ±2 cm. At the 2-cm level there are several comparable error sources, so that it simply does not make sense to invest a large amount of resources in the reduction of any single error source. Keep in mind that the 2-cm vapor delay accuracy refers to a differential measurement, so that the accuracy of an individual measurement should be $2/\sqrt{2}$ cm. We would like the precision of the vapor measurement to be a factor of 3 or 4 better in the hope that the increased precision could be used to spot systematic effects. Hence the overall system requirement for the WVR is that it measure vapor delay with accuracy of ±1.5 cm and precision of ±0.4 cm. Our problem in 1978 was to convert this requirement on system performance into a general set of design specifications.

As a response to a directive from the JPL Program Office for the Crustal Dynamics Project we formed a design team to review the design specifications for a water vapor radiometer. The conclusions and recommendations of this team were issued as a JPL internal report, which was written in the very early stages of construction and became the engineering specifications document. Table 1 summarizes the specifications of the water vapor radiometers.

A. Physical Characteristics and Environment

Since we started with a stock of existing parts the physical characteristics of the WVR were somewhat predetermined. The physical characteristics of units R01 and R04 to R08 are listed in Table 1. Units R02 and R03 have slightly larger volume but more or less the same physical characteristics. The environmental factors were specified from consideration of the meteorological conditions for both the mobile and fixed antenna sites that were under consideration by the Crustal Dynamics Project. At temperatures below -10°C it was felt that the atmospheric vapor content would be very small and hence there would be little need for the vapor correction. The WVRs will survive temperatures as low as -40°C but below -10°C it becomes increasingly more difficult for the internal heaters to thermally stabilize the electronics. Similarly, at wind speeds above 65 km/hr the VLBI antenna would probably shut down. At wind speeds higher than 95 km/hr it is recommended that the WVR be stowed in the horizontal position in order to present the minimum surface to wind loading. A particularly irksome problem that was not solved was the problem of dew accumulation on the cover of the horn antennas.

B. Operating Frequencies

One of the critical specifications in the WVR design is the choice of operating frequencies. This is because the water vapor line centered at 22.235 GHz is pressure broadened. Thus the line profile will depend on the altitude distribution of the vapor. A given amount of vapor that was concentrated at low altitude would produce a wide, flat profile relative to the same amount of vapor that was concentrated at high altitude. Most of the vapor signal is produced at 22.235 GHz but this is also the frequency that is most sensitive to the shape of the line. However, if we pick a frequency on the wing of the line, e.g., between 20 and 21 GHz, we can minimize this sensitivity to vapor height (Ref. 14 and 15).

The components of the NEMS (unit R01) radiometer operated at 22.2 and 31.4 GHz, and the two Sense Systems radiometers operated at 21.0 and 31.4 GHz. Preliminary bench tests indicated that the NEMS components could possibly be used as low as 20.7 GHz. There is a decided advantage of having all WVRs operate at identical frequency pairs, so we decided to standardize on 20.7 GHz as the vapor sensitive channel for all new WVRs and attempt to retune the existing components.

C. Frequency Stability

The specification of frequency stability is important because the vapor channel operates on the part of emission line where the rate of change of brightness temperature with respect to frequency is largest. The frequency will change because the Gunn diode local oscillator is temperature-sensitive and the WVR enclosure does not act as a perfect oven. The sensitivity is approximately 3 MHz/°C and since temperature changes of ±4°C inside the WVR are possible, this implies frequency shifts of ±.012 GHz. At a precipitable vapor content of 2 gm/cm^2 the rate of change of brightness temperature with respect to frequency is 3.3 K/GHz, so that 0.04 K errors are possible in the presence of moderate amounts of vapor. These errors are below the quantization level of the A/D converter for most observing conditions.

D. Bandwidth and Integration Time

The bandwidth specification, like the operating frequency of 20.7 GHz, was set by equipment in-hand. Both the NEMS unit and the two Sense Systems units are double sideband receivers with an IF passband from 10 to 110 MHz. The Dicke switch rate is 1000 Hz on all of the radiometers. The minimum integration time is set by a lowpass filter on the output of the synchronous detector whose characteristics were based on three considerations. First, the time constant should be long enough to span many cycles of the Dicke switch and thereby average out transients and any short term dithering in the switch reference frequency. Second, the time constant should be large enough to reduce the random noise fluctuations to a value that is several times the quantization level of the analog-to-digital converter. Third, the time constant should not be so large as to impose tedious wait states between changes of the input. We chose a lowpass filter with an equivalent time constant of 100 millisec and thereby average 100 cycles of the Dicke switch. The rms fluctuation level is approximately 0.4 K compared to a quantization level of 0.1 K. The wait state after a mode change is determined by the time it takes the previous level to decay to less than the quantization level, which for our design is 9 time constants or 0.9 sec. This delay is enforced in the controller software – the WVR simply will not respond for 0.9 sec after a mode change. The effective integration time can be lengthened by software averaging techniques.

E. Antenna

Ideally, one would like the antenna beamwidth of the WVR to be comparable to the beamwidth of the radio telescope to be calibrated. However, as indicated previously, this restricts the use of the WVR in other applications. In addition, a comparable WVR beam would entail considerable cost either as hardware or in development, in that it would mean a WVR aperture whose diameter is comparable to the radio telescope with all of the attendant problems of pointing, spillover, etc. These problems are solvable given enough time and money, but this is unnecessary in our application.

We chose to use a horn antenna for the WVR that has a relatively broad beamwidth (7 degrees, full width at half maximum) for three reasons: (1) it has virtually no sidelobes, (2) the dimensions could be easily scaled to give the same beamwidth at both operating frequencies, and (3) the temporal/spatial resolution of the broad beam was more than sufficient in our applications. The beam pattern for this horn is shown in Fig. 4 taken from Ref. 16. In order to have a WVR beam that was comparable to that of the 64-m antenna operating at a 3.8-cm we would need a 16-m aperture. We could either use a separate 16-m paraboloid for the WVR or we might consider mounting the WVR in such a way as to utilize some or all of the 64-m aperture. In either case we would have to devote considerable engineering effort toward minimizing the problems of sidelobes and spillover that produce serious systematic error in the delay determination. Furthermore, since we use a variety of radio telescopes in our application we would require a custom WVR aperture or feed for each installation. Clearly this is impractical – if we need eight WVRs perhaps a single design is most cost effective. However, if one is to use a composite design, then the question that arises is how do we relate the output of the WVR to the output of the radio telescope when they have unequal beams?

Formally, there is an important distinction between the antenna temperature (which is what the WVR measures) and the sky brightness temperature (which is what we wish to measure). The antenna temperature T_a (neglecting losses) is given by a convolution of the brightness temperature distribution $T_b(\theta, \phi)$ with the antenna beam pattern $P(\theta, \phi)$ as,

$$T_a \sim \int T_b(\theta, \phi)\, P(\theta - \theta_0, \phi - \phi_0)\, d\Omega \qquad (5)$$

where θ, ϕ are spherical coordinates and (θ_0, ϕ_0) is the pointing direction. If the beam pattern has unwanted responses in directions other than the pointing direction then we must correct for them. A typical sky brightness temperature of 30 K would be considerably corrupted by a 100 K cloud or the 300 K earth in a sidelobe even if the sidelobe responses were 20 dB down from the main beam. The virtue of having an antenna beam with no sidelobes (i.e., very high main beam efficiency) is that we can equate the antenna temperature to the brightness temperature (except for a small pointing correction) and save a great deal of data "massaging."

When we ask how the vapor affects a large radio telescope we must keep in mind that the beam of the radio telescope

takes a relatively large distance to form. The extent of the near field of an aperture is

$$L_{nf} \sim D^2/\lambda \tag{6}$$

where D is the diameter of the aperture and λ is the observing wavelength. This quantity is tabulated in Table 2 for some of the antennas used in our applications. Since the scale height of water vapor is typically 2 km, this means that most of the vapor is in the near field of a large radio telescope. Thus fluctuations in phase for the radio telescope are determined by the vapor inhomogeneities that pass through a cylindrical column of length L_{nf} and diameter D.

Let us assume that the water vapor exists in the form of "blobs" that are randomly distributed in size. If we sample equal volumes of atmosphere containing $N_1, N_2, \cdots$ etc., then we would expect to find N blobs on the average with an rms variation of $\sqrt{N}$. We would obviously expect less variation if we sampled with a large volume as compared to sampling with a small volume. If we normalize N to be the number of blobs per unit area, then the average value will be independent of sampling volume but the rms variations about the average will be a function of the sampling volume. Thus we can roughly estimate the difference in fluctuation between the WVR and radio telescope by simply computing the average vapor contained in the two beams. If we will assume that on the average the water vapor is exponentially distributed with scale height H_0, and the WVR beam is approximated by a cone of full-width β, then it is straightforward to calculate the ratio R of the volume of vapor in the WVR beam to the volume of vapor in the near field of the radio telescope,

$$R = V_{wvr}/V_{cyl} = 8[(H_0/D)\tan(\beta/2)]^2 \tag{7}$$

This ratio is shown in Table 2 using the 7-deg beamwidth of the WVR. If we neglect instrumental noise then we would expect the ratio of the fluctuations for the WVR to the fluctuations from the radio telescope to vary as the square root of R. The WVR, since it samples a larger volume, will vary less, but on the average it will determine the correct delay for the radio telescope.

An alternate way to view this problem is to note that Eq. (5) is a function of time. The brightness temperature describes the two-dimensional projection of an assemblage of water vapor inhomogeneities that are constantly rearranged by winds aloft. Thus the quantity T_a is really a time series. If we had a pencil beam, i.e., $P(\theta, \phi)$ were a delta function, then the time variations of T_a and T_b would be identical. The fact that we have a beam of finite width that is convolved with T_b implies that the antenna acts as a lowpass filter by spatially averaging the details of the sky brightness distribution. Therefore, we expect the output of the WVR to be a smoothed representation of the output from the radio telescope. On very short time scales the radio telescope may exhibit fluctuations that the WVR will not detect.

The calculation of the time scale that relates the WVR to radio telescope fluctuations is quite complex, involving the geometry and the three-dimensional spectrum of vapor inhomogeneities. We shall resort to a more intuitive approach. Consider that at the zenith the width of the WVR beam is approximately

$$D_w = 2H\tan(\beta/2) \tag{8}$$

where H is the height. For a height of 2 km (the nominal scale height of water vapor) and a beam width of 7 deg we calculate D_w = 244 m or roughly 10 times the near field width from a 25-m radio telescope. For a given blob diameter D and radio telescope diameter D_R, we can distinguish three different regimes. Regime 1: $D < D_R$, the ratio of the time that the blob spends in the WVR beam to the time it spends in the radio telescope beam is $T \sim D_w/D_R$. Regime 2: $D_R < D < D_w$, the time scale is $T \sim D_w/D$. Regime 3: $D > D_w$, the ratio of the times becomes $T \sim 1$. Thus in this example the very small blobs of vapor will spend about 10 times longer in the WVR beam as they do in the radio telescope beam, but as the size of the blob grows the ratio of time spent in the two beams approaches unity. If we further assume that the horizontal and vertical dimensions of the blob are roughly equivalent then it follows that the small blobs will cause small phase perturbations and large blobs will cause large perturbations. The WVR will not "see" the short-period fluctuations in the radio telescope output that are due to water vapor but it can detect the larger long-term effects. In reality, nature is not nearly so simple and all that can be safely said is that there is a rough equivalence between the spatial averaging of the WVR and temporal averaging from the radio telescope.

F. Calibration

Two types of calibration are required for the WVR: (1) a frequent calibration of the relative gain of the instrument, and (2) a less frequent calibration of the absolute gain. The reference load of the Dicke switch is kept at the same temperature as the rest of the electronics. This means that the Dicke receiver is not fully stabilized (e.g., see Ref. 11) and we are susceptible to gain changes. Determination of the relative gain is accomplished by setting internal switches in the WVR so that the input of the Dicke receiver is connected to either of two waveguide terminations. One termination is kept at an elevated temperature (100°C) and is called the hot load while the other is kept at the same temperature as the rest of the electronics (43°C) and is called the base load. The physical

temperature of these loads is measured with thermistors and denoted by *TH* and *TB* respectively. The output of the receiver is digitized and presented to the user as a number *N* that we shall term "counts." In order to determine an unknown antenna temperature *TA* we can (in principle) go through the observing sequences – hot load, base load, antenna – and observe the outputs *TH, TB, NH, NB*, and *NA*. For an ideal radiometer the antenna temperature is simply

$$TA = TB + [(TH - TB)/(NH - NB)]\ (NA - NB) \quad (9)$$

where the quantity in square brackets is called the relative gain or simply the gain of the instrument and is expressed in units of kelvin/count. For all of the WVRs, the value of the gain is approximately 0.1 K/count and is determined by the product of the gains from all circuit elements extending from the Dicke switch to the analog-to-digital converter. Figure 5 illustrates the typical fluctuations in the gain from one of the WVR channels. We plot the relative gain (i.e. by subtracting out the average) vs time for a 40-hour period. A diurnal variation of ±4% is quite obvious and is due primarily to temperature changes inside the microwave package. Superimposed on the diurnal variation are short-term fluctuations due primarily to radiometer noise which can be reduced by averaging or smoothing.

Equation (9) describes an ideal radiometer. A real instrument suffers various shortcomings such as attenuation, less than perfect switch isolation, reflections, etc. The calibration of absolute gain involves finding the correction factor that puts Eq. (9) closer to the absolute temperature scale. One of the procedures that can be used to find the instrumental correction factor is called a "tip curve"; it is used to derive a correction to the hot load. Let us assume that we can rewrite Eq. (9) for a real radiometer as

$$TA = TB + [TH - TB + \Delta TH]\ N' \quad (10)$$

where $N' = (NA - NB)/(NH - NB)$ is the normalized count in the antenna mode, and ΔTH is the hot load correction. The brightness temperature of the sky can be written

$$T_b = T_c e^{-\tau} + T_m(1-e^{-\tau}) \quad (11)$$

where $T_c = 2.9$ K is the cosmic blackbody background, T_m is the mean radiating temperature of the atmosphere, and τ is the opacity. The mean radiating temperature exhibits some seasonal and site variations but with a reasonable degree of approximation we can assume that it is constant and equal to 275 K. For a stratified atmosphere the opacity can be expressed as,

$$\tau = \tau_0(AM) \quad (12)$$

where τ_0 is the zenith opacity and $AM = 1/\sin$ (elevation) is the air mass. Suppose we make a series of observations, first observing the internal loads to get *TB, TH, NB*, and *NH*, and then moving to different elevation angles to get NA_1, NA_2, · · · etc., at positions AM_1, AM_2, · · · etc., and assume that $TA = T_b$. Equations (10), (11), and (12) can be combined to give,

$$N_{i'} = [T_M + T_B + (T_c - T_m)\exp(-\tau_0 AM_i)]/(TH - TB + \Delta TH) \quad (13)$$

Thus we have expressed the observable from the WVR as the dependent variable in terms of the independent variable AM_i and the two parameters τ_0, and ΔTH. Given two or more observations at different AM_i it is straightforward to solve for τ_0 and ΔTH that are "best" in the least squares sense. Figure 6 shows tip curve data taken with WVR-R07 (31.4 GHz) located at Goldstone in May 1981. All WVRs are calibrated in this manner prior to shipment. In addition, the temperature scale of each radiometer channel is checked by observing hot and cold aperture loads, which serves as a consistency check.

The proof of WVR performance lies in a comparison of the WVR with some independent (and one would hope more accurate!) technique of measuring vapor path delay. The most convenient comparison technique is to use a radiosonde to provide a vertical profile of temperature and relative humidity that can be integrated to give an estimate of the zenith path delay which we then compare with the delay estimate from the WVR that is observed at the zenith. Figure 7 shows two such comparisons, the first done in May 1974 and the second from May 1975 that was reported in Ref. 5. Figure 8 shows previously unpublished data taken at Pt. Mugu, California in 1976, and Fig. 9 shows the histogram of the residuals for this experiment. During the Pt. Mugu experiment we had an instrumented aircraft fly various slant paths up to a maximum altitude of 3 km, which provided a larger range of path delay estimates than are normally obtained from radiosondes. This data is shown in Fig. 10.

The rms residuals from these comparisons are 1.6 cm from 1974, 1.1 cm from 1975, 1.5 cm from 1976 WVR/radiosonde, and 1.4 cm from 1976 WVR/aircraft (excluding data at 10 deg elevation). If the two techniques are truly independent then we expect the rms residual to be the root-sum-square of the error from each technique. If we take the average rms residual to be 1.5 cm, and assume that the radiosonde has a 10% accuracy, the average path delay to be 1.0 cm, then we infer the accuracy of the WVR to be 1.1 cm.

The WVR used in the experiments just described operates at 22.2 and 31.4 GHz. Unfortunately none of the new WVRs

have undergone such comparison. If anything, the older radiometers should be noisier due to the greater sensitivity to the vertical distribution of vapor. Guiraud et al. in Ref. 17 report a WVR/radiosonde comparison for a WVR that operates at 20.6 and 31.6 GHz and infer a WVR accuracy of 0.5 cm. We hope to demonstrate comparable performance with the new WVRs.

The instrumental correction factor should be constant for long periods of time (e.g., years). There are circumstances that could cause it to change slowly or dramatically. For instance, it is possible that the waveguide walls could deteriorate slowly in time due to atmospheric constituents. If the enclosure is leaking and there is a sudden change from warm, damp conditions to cold conditions, then liquid water or ice could form in the waveguide or switches or on the cover of the horn antenna. In either case the performance of the instrument will change and the predetermined value of ΔTH will not be valid. It is recommended that tip curves be performed periodically and the results kept as a history of the instrumental performance.

G. Temperature Control

The quantity that correlates most strongly with gain variations is temperature, so that it is important that the WVR have enough thermal inertia to resist sudden changes in temperature. Conversely, the gain should be monitored on time scales shorter than the time scale for real temperature changes. The important specification is the restriction that the physical temperature of any load must not change by more than the quantization level during the time it takes to measure the gain. Thus, the specification ±0.1°C/minute assumes that it will never take longer than one minute to measure the gain.

Almost all of the microwave components are thermally connected to a large aluminum mounting plate. A mercury thermostat controls strip heaters attached to this plate and regulates its temperature to 43°C. A small fan circulates air around the few components that are not attached to the plate. The entire microwave package is enclosed by a sheet metal box that is lined with styrofoam and provides a thermal attenuation of approximately 6-7 dB. The box is attached to the positioner with a base plate made from a thermally insulating material. Thermal baffles are mounted on standoffs on the four sides of the box that expose the largest area. These baffles, which are covered with a paint that has high reflectivity in the infrared, were found to be necessary for summer operation in desert-type environments.

Figures 11 and 12 show the warmup characteristics of the two waveguide terminations (i.e. the hot and base loads). Typically, the hot load requires 1.5 to 2 hours to thermally stabilize and will remain constant to ±0.2°C thereafter. The base load, which is representative of the remainder of the electronics package, takes up to 3 hours to reach quasi-equilibrium. Figure 13 shows the typical diurnal variation of the enclosure temperature, which correlates very well with the gain variations.

H. Positioning Module

The specifications for the positioner follow from the requirement that the WVR point along the same line of sight as the radio telescope that is being calibrated. This is most easily done with an Az/El mount and conversions from right ascension/declination done in software if necessary. Due to the 7-deg bandwidth of the horn antennas, we have not included a capability for tracking – only pointing. Also note that the pointing capability is ±1.0 deg. but the readout precision is ±0.1 deg. Analysis of the pointing sensitivity indicates that positioning errors of ±0.1 deg will give worst-case errors of 0.5 K in brightness temperature and 3 mm in the path delay in high opacity/low elevation angle conditions. Using these instruments in a typical VLBI experiment one would point to within ±1 deg of the line of sight of the radio telescope (keeping 10 deg away from obstructions). Then one would request the data necessary to calculate the path delay, and note the actual position of the WVR so that the path delay could be mapped to the correct line of sight by assuming a cosecant elevation angle scaling.

The slew rate of the positioner even for the two "slow" units is generally much faster than the associated radio telescope. This allows the possibility of more complex observing strategy with the WVR than simply following along behind the radio telescope. Details of the operation of the positioner will be given in a later paper of this series.

I. Control and Interface Module

This module consists of a local control/monitor panel and microcomputer. Using the local control panel the user can manually point the WVR, switch modes, or monitor any of the signal lines from either the microwave or positioner modules. These signals are displayed on a built-in digital voltmeter and are available via BNC jacks on the panel in order to drive a chart recorder. The control panel is intended primarily to assist in diagnosis of problems. In normal operation the control panel is switched to the REMOTE position and all control and data acquisition is exercised by the microprocessor. The interface to the microprocessor is set by the requirement of compatibility with the MK III data acquisition system. In early talks with colleagues at Goddard Space Flight Center and at the Haystack Observatory it was decided that the WVR would simply be treated as one of several devices on a daisy-chain type of serial interface. This interface has come to be known as the MAT (Microprocessor ASCII Transceiver) bus.

Originally it was believed that the new RS422/423 interface standard would be necessary to implement the long lines to the WVR that we thought might occur at some installations. Unfortunately, reliable components to implement the RS422/423 standard were not available in time to be implemented. A simple three wire RS-232 is now in use with short-haul modems for the WVR interface lines.

The baud rate of the WVR is set to any standard rate from 75 to 19,200 baud by a combination of software and jumper changes on the microcomputer board. At the present time it is set to 9600 baud. Implementation of the operating modes and command/respond sequence is primarily a matter of sufficient software in the microprocessor. In the current version of this software only the OPERATE mode has been implemented along with a set of primitive commands. Details of this software will be discussed in a later paper. The microcomputer contains an analog I/O subsystem that is used to digitize the various analog signals from the mocrowave package and the positioner. Our desire for 0.1 deg of position resolution dictated the choice of a 12-bit A/D converter (i.e., $2^{-11} > 0.1/360 > 2^{-12}$). Similarly, the quantization of the physical and brightness temperature measurements is 0.1 K. As indicated previously, the fluctuation level from the radiometer is on the order of 0.4 K. It is possible to average many samples in order to reduce these fluctuations. However, Clark (Ref. 18), has pointed out this must be done with caution if one attempts to reduce the fluctuations below the quantization level.

VI. In Retrospect

Table 3 summarizes the hardware costs and time expended as a result of our work on the WVRs. Hardware costs are referred to epoch October 1981 and for the most part must be inflated to the current date. An exception to this is the microprocessor hardware where many components are being reduced in price. The hardware, assembly, testing, and calibration costs are listed on a per unit basis. The development of the algorithm, microprocessor control software, and the data acquisition software is summarized as a total effort. The final accounting of hardware cost and assembly time was very close to our original estimates for this task in spite of severe price inflation. This was due largely to the fact that we were more efficient in assembly than originally estimated. Having several WVRs under construction meant that some jobs could be done on a "production line" basis and there were always lots of little jobs that kept everyone busy.

The software part of the WVR task cost a great deal more than we originally estimated. There were essentially three reasons for this overrun. First, purchase and delivery of the JPL MK III data acquisition system was delayed, which meant that we had to purchase additional hardware for host computers other than the MK III computer. These additional microcomputers were intended to serve as "host" machines and were not in our original budget. In order to save dollars we purchased lowest-bidder type of equipment, which was a serious mistake. We saved a few dollars on the hardware but spent much more later in maintenance costs and schedules that had to be slipped because equipment was not working. The second reason for the software overrun was due to the fact that we simply underestimated the amount of system-level support we would need to keep several development systems running. The third and major reason for the overrun was due to the personnel turnover among the people working on the software. Over the three years of the task there were eight people who worked on the software or algorithm development. All worked part time and five left after several months on the job – an extremely inefficient way to develop software.

Had we realized at the time we started building these instruments that we would construct eight of them, we probably would not have used the conventional Dicke design. One can imagine a spectrum of design possibilities that range from a fully compensated Dicke radiometer utilizing full digital control and data acquisition to a single-horn total power instrument. The goal in any redesign effort should be to lower the parts count, thereby decreasing the hardware cost, reducing assembly time, lowering weight, size and power requirements, and increasing instrumental stability. At some point in the design spectrum one is inevitably faced with the possibility of cost/performance tradeoff that can limit the applicability of the instrument. It is our educated guess that the cost of the WVR could be reduced by 15-30% by simply reengineering the current design but keeping the same overall characteristics of the current instruments. Potential cost reductions of a factor of 2 are possible but entail some technical risk that would require a design study at the least and possibly the construction and testing of a prototype.

Acknowledgments

It is a pleasure to acknowledge the assistance of colleagues who, at various times, have contributed to this task. Pete MacDoran, Don Trask, and Jim Johnston provided support and encouragement at critical times. Bruce Gary and Joe Waters have generously shared their insight into the techniques of remote sensing. Bob Clauss has made valuable comments regarding both the real and the theoretical behavior of the instrumentation. Al Banisch handled the engineering on the first WVR (Unit R01). Dave Peterson has helped with everything from fabrication to calibration. Rick McKinney performed a valuable service with his part of the testing and the fix for some of the problems that were uncovered. Bill Sinclair wrote the first two versions of the controller software and helped with some of the system support software. Kwok Ong wrote the nucleus of the data acquisition software and helped with system support and data analysis. At different times, Scott Claflin, Robin Hastings, and Henry Fliegel have provided much needed help with the algorithm development. Bob Miller helped with software development and hardware testing and calibration.

References

1. Smith, E. K., and Weintraub, S., "The Constants in the Equation for Atmospheric Refractive Index at Radio Frequencies," *Proc. IRE*, V41, pp. 1035-1057, 1953.

2. Gold, T., "Radio Method for the Precise Measurement of the Rotation Period of the Earth," *Science*, V167, p. 302, 1967.

3. Shapiro, I. I., and Knight, C. A., "Geophysical Applications of Long Baseline Interferometry," in *Earthquake Displacement Fields and the Rotation of the Earth* (Mansinha, Smylie, & Beck, eds), Reidel Publ., Holland, pp. 284-301, 1970.

4. Ong, K. M., MacDoran, P. F., Thomas, J. B., Fliegel, H. F., Skjerve, L. J., Spitzmesser, D. J., Batelaan, P. D., and Paine, S. R., "A Demonstration of a Transportable Radio Interferometric Surveying System with 3-cm Accuracy on a 307-m Baseline," *J. Geophys. Res.*, V81, pp. 3587-3593, 1976.

5. Winn, F. B., Wu, S. C., Resch, G. M., Chao, C. C., von Roos, O. H., and Lau, H., "Atmospheric Water Vapor Calibrations: Radiometer Technique," *DSN Progress Report 42-32*, Jet Propulsion Laboratory, Pasadena, Calif., pp. 38-49, Apr. 15, 1976.

6. Moran, J. M., and Penfield, H., "Test and Evaluation of Water Vapor Radiometers and Determination of Their Capability to Measure Tropospheric Propagation Path Length," SAO final report on Contract NAS5-20975 (June 1976) available from National Technical Information Service, Springfield, Va., 1976.

7. *Atmospheric Water Vapor*, ed. Deepak, Wilkerson, and Ruhnke, Academic Press, New York, 1980.

8. *Remote Sensing of the Troposphere*, ed. V. E. Derr, U. S. Government Printing Office, Washington, D. C., 1972.

9. Staelin, D. H., "Measurements and Interpretation of the Microwave Spectrum of the Terrestrial Atmosphere near 1-cm Wavelength," *J. Geophys. Res.*, V71, pp. 2875-2882, 1966.

10. Westwater, E. R., "The Accuracy of Water Vapor and Cloud Liquid Determination by Dual-Frequency Ground-Based Microwave Radiometry," *Radio Science*, V13, pp. 677-685, 1978.

11. Tiuri, M. E., "Radio-Telescope Receivers," in *Radio Astronomy* (by J. D. Kraus), McGraw-Hill Book Co., New York, 1966.

12. Rogers, A. E. E., "Very Long Baseline Interferometry with Large Effective Bandwidth for Phase-Delay Measurements," *Radio Science*, 5, pp. 1239-1247, 1970.

13. Resch, G. M., "Water Vapor – The Wet Blanket of Microwave Interferometry," in *Atmospheric Water Vapor* (Deepak, Wilkerson, and Ruhnke, eds), pp. 265-282 Academic Press, New York, 1980.

14. Westwater, E. R., "An Analysis of the Correction of Range Errors Due to Atmospheric Refraction by Microwave Radiometric Techniques," ESSA Technical Report IER 30-ITSA30, available from National Technical Information Service, Springfield, Va., 1967.

15. Wu, S. C., "Optimum Frequencies of a Passive Microwave Radiometer for Tropospheric Pathlength Correction," *IEEE Trans. Ant. & Prop.*, AP-27, pp. 233-239, 1979.

16. Janssen, M. A., Bednarczek, S. M., Gulkis, S., Marlin, H. W., and Smoot, G. F., "Pattern Measurements of a Low-Sidelobe Horn Antenna," *IEEE Trans. Ant. & Prop.*, AP-27, pp. 551-555, 1979.

17. Guiraud, F. O., Howard, J., and Hogg, D. C., "A Dual-Channel Microwave Radiometer for Measurement of Precipitable Waver Vapor and Liquid," *IEEE Trans. Geoscience Elect., GE-17*, pp. 129-136, 1979.

18. Clark, B. G., "The Effect of Digitization Errors on Detection of Weak Signals in Noise," *Proc. IEEE*, V61, pp. 1654-1655, 1973.

Table 1. Water vapor radiometer specifications

(1) Physical characteristics	Weight, kgm	Volume, m^3	Power, W
Microwave package	45	0.12	300–600
Positioner	34	0.074	0–450
Control module	26	0.15	120
(2) Environmental			
Operating range			
Ambient temperature	−10 to +50°C		
Wind speed	up to 65 km/hr		
Relative humidity	0 to 95% or until liquid water precipitates onto the horn cover		
Survivability			
Ambient temperature	−40 to +60°C		
Wind speed	up to 160 km/hr in stowed position		
Relative humidity	100%, sealed from rain and dust		
(3) Microwave module			
Operating frequencies	20.7 and 31.4 GHz		
Frequency stability	±12 MHz over operating range		
RF bandwidth	200 MHz		
IF bandwidth	100 MHz		
Integration time	software selectable in steps of 0.1 sec		
Signal range	3 to 400 K		
Antenna beamwidth	7° (full width at half power)		
Beam efficiency	>99.9% for ±15° around beam center		
Calibration	supplied by two waveguide terminations held at fixed temperatures and supplemented with tip curve observations		
Base load	315 K		
Hot load	370 K		
Temperature stability	>±0.1 K/min		
(4) Positioner			
Coordinates	azimuth and elevation		
Range	0 to 355° in Az, 5 to 175° in El		
Slew rate	> 1.5 deg/sec (both axis)		
Position accuracy	1° both axes		
Readout accuracy	0.1° both axes		
(5) Control and interface module			
Operating modes			
(a) Local	all data and control lines available for monitoring by built-in digital voltmeter		
(b) Remote			
Interface	RS-232, twisted pair of cables		
Baud rate	110 to 19200 baud, selectable by software and hardware jumpers		
Protocol	compatible with MAT[a] bus		
Data storage	temporary storage only, mass storage is the responsibility of the host computer		

[a]MAT = Microprocessor ASCII Transceiver used as the control/communicator standard in the HaystackGSFC Mark III data acquisition system.

Table 2. Extent of the near-field and beam volume ratios for WVR and radio telescope

Diameter, m	Frequency, GHz	L_{nf}, km	R	$\sqrt{R}$
64	8.4	108.00	29.2	5.4
64	2.3	32.00		
40	8.4	42.00	74.8	8.6
40	2.3	12.30		
25	8.4	16.40	191.5	13.8
25	5.0	10.40		
25	2.3	4.80		
9	8.4	2.10	1477.9	38.4
9	2.3	0.60		
4	8.4	0.40		
4	2.3	0.01		

Table 3. Cost summary

A. Cost per radiometer (as of Oct. 1981)

Components	K$	Tasks	Man-month
Ferrite switches	7.3	Fabrication	3.0
LO/mixer/I.F.	8.5	Assemby and wiring	4.0
Horn antennas	3.1	Bench testing	3.0
Waveguide components	1.0	Engineering tests	0.8
Power supply	1.7	Calibration	2.0
Detectors	0.1		
Temp sensors and control	0.4		12.8
Enclosure (microwave)	0.6		
Misc. components	1.2		
Control panel	0.8		
Microprocessor	4.5		
Positioner	2.8		
Cables and connectors	0.5		
	$32,500.0		

B. Support tasks

Task	Man-years
Controller software (3 versions)	1.2
System support	0.8
Data acquisition S/W	1.0
Environmental test	0.2
Algorithm development	2.0
	5.2 MY

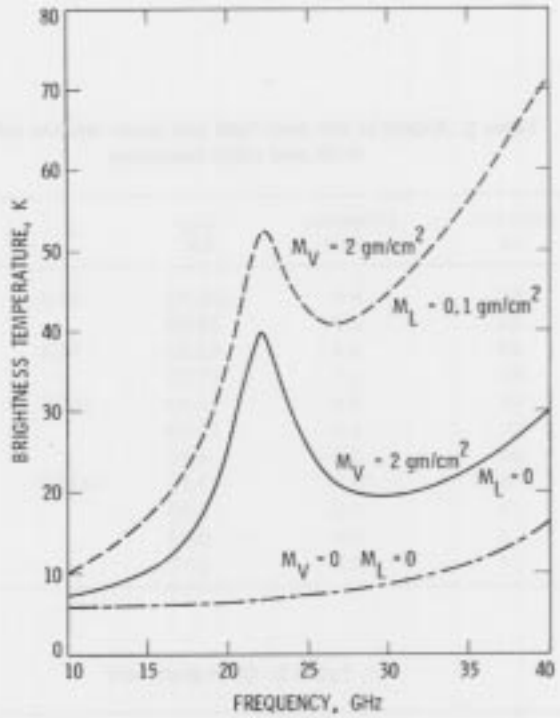

Fig. 1. Zenith brightness temperature of the atmosphere between 15 and 40 Ghz

Fig. 2. Photograph of the three WVR modules (cover removed from the microwave package)

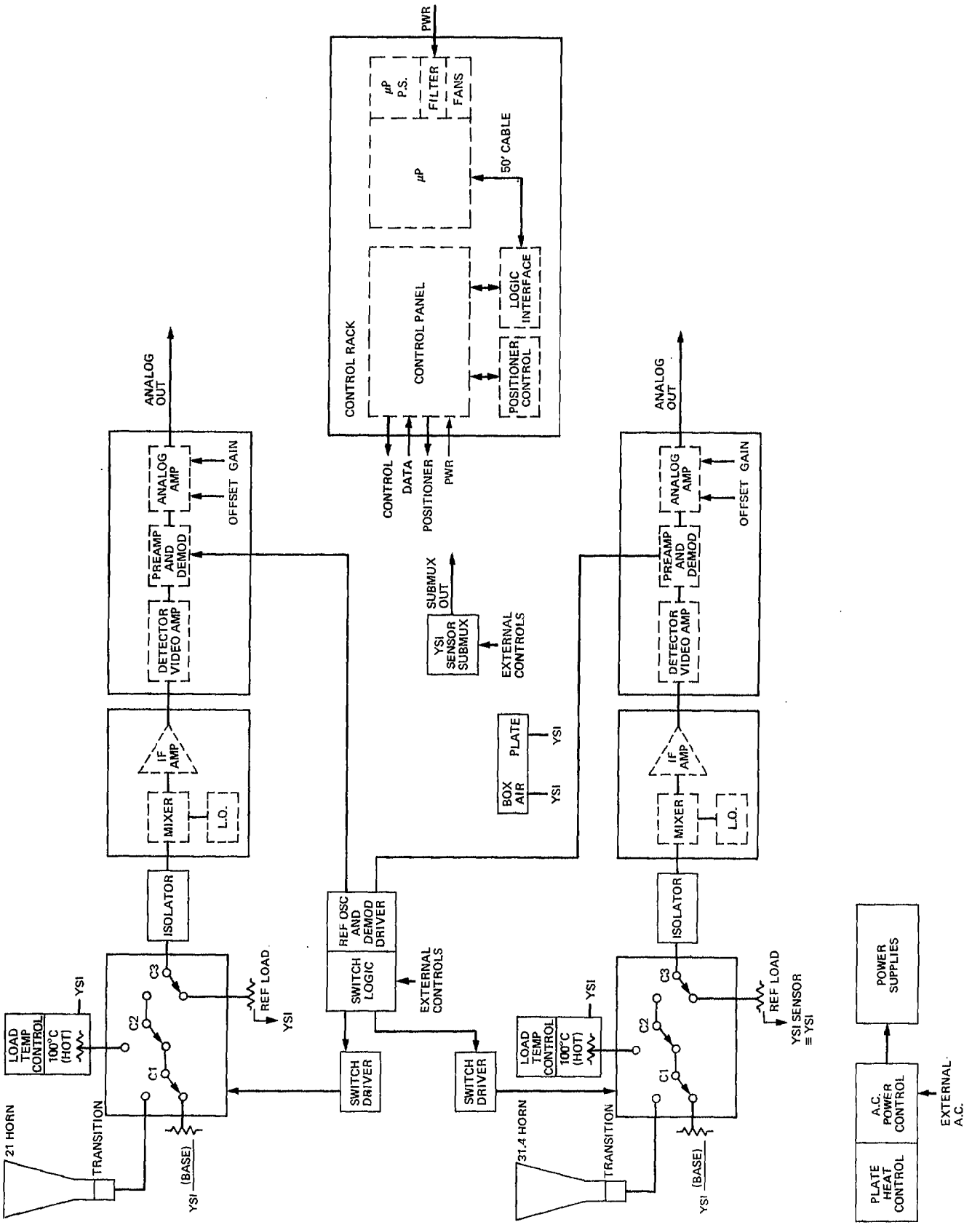

Fig. 3. Block diagram of the WVR

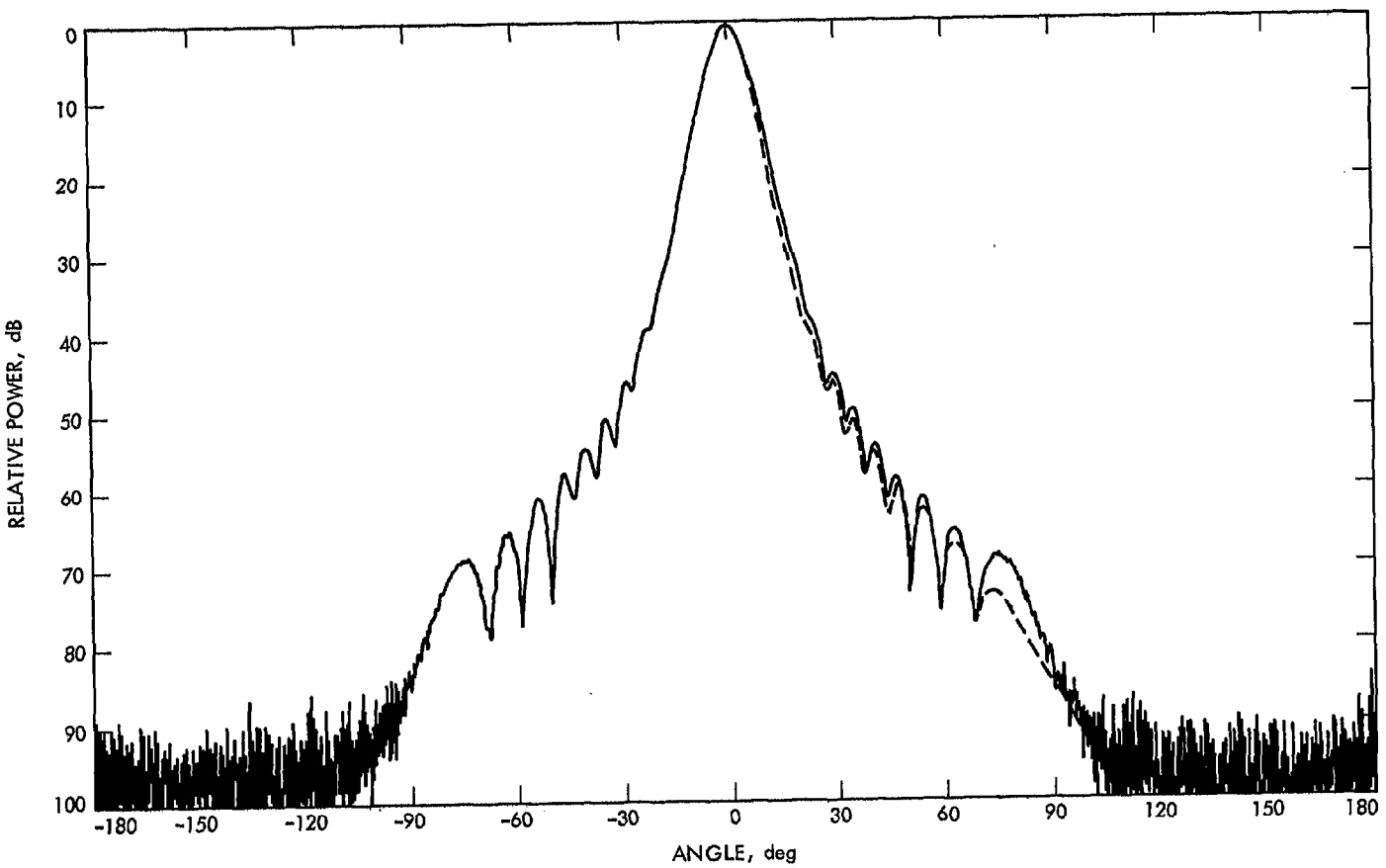

Fig. 4. Antenna beam pattern of the WVR horn antenna

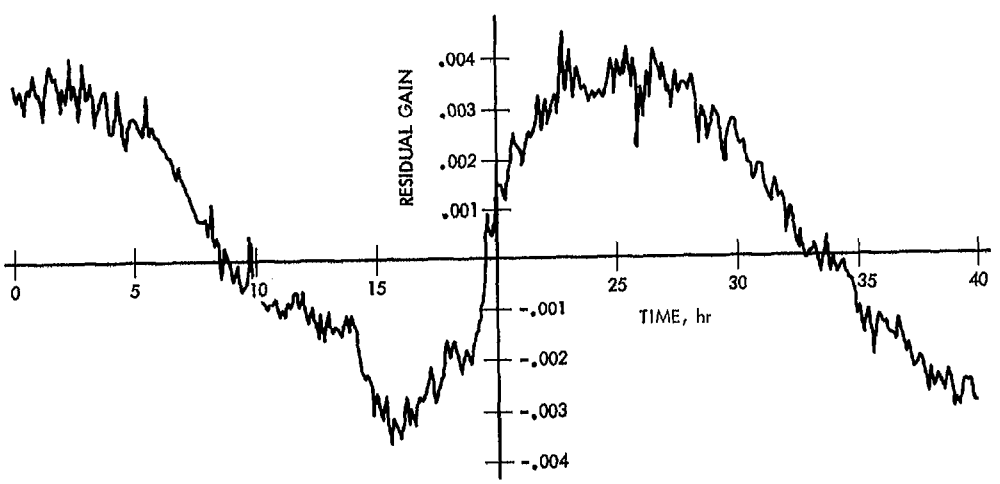

Fig. 5. Gain of one of the WVR channels vs time

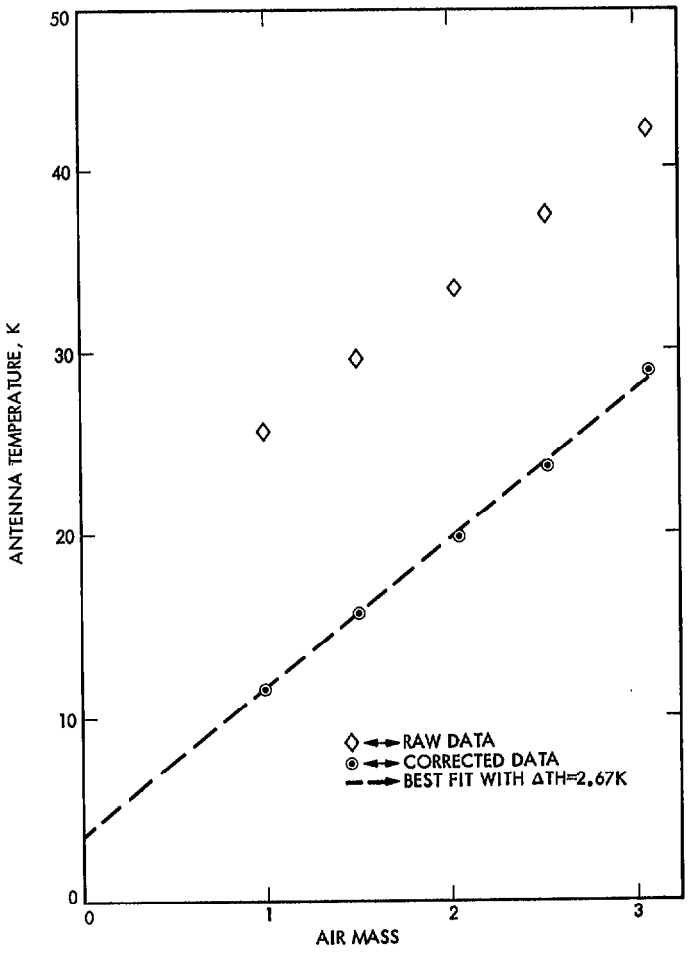

Fig. 6. Tip curve determination of the hot load correction

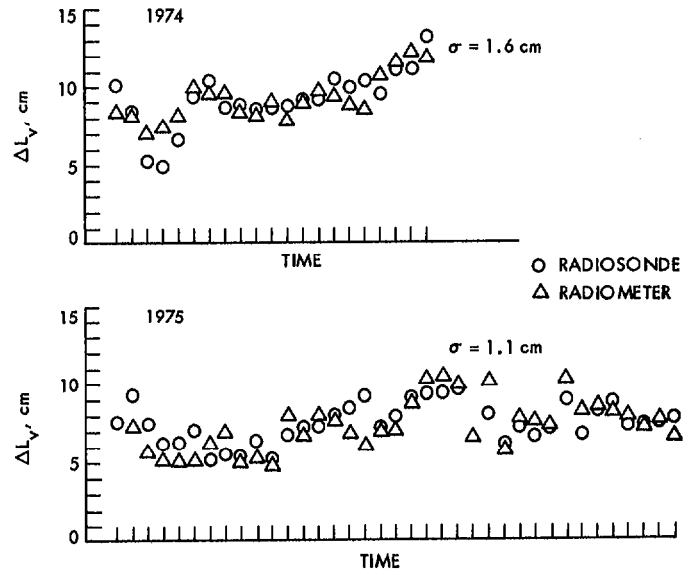

Fig. 7. Comparison of path delay as determined by radiosonde and WVR (El Monte, 1974 and 1975)

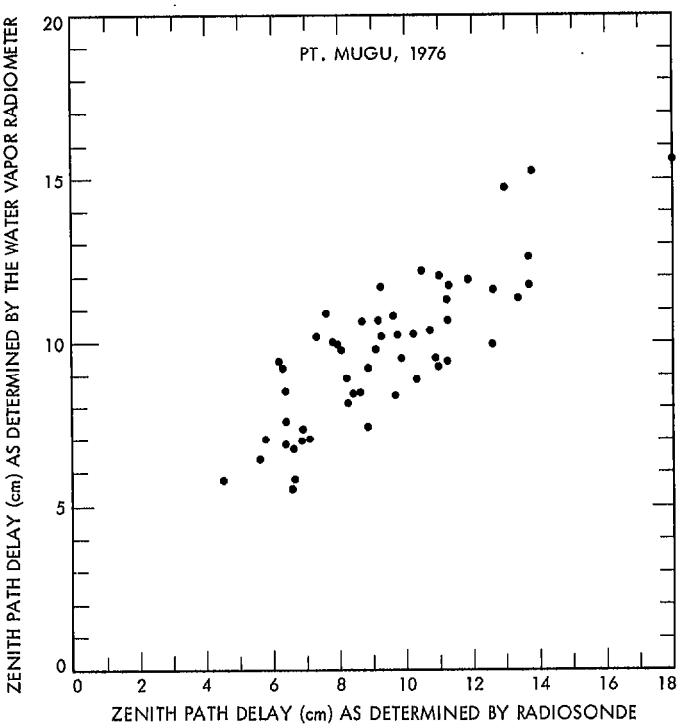

Fig. 8. Comparison of path delay as determined by radiosonde and WVR (Pt. Mugu, California, 1976)

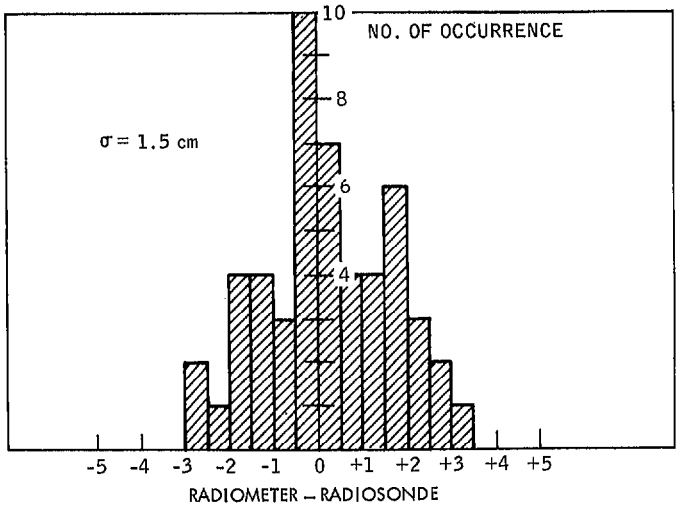

Fig. 9. Histogram of path delay residuals from the Pt. Mugu data

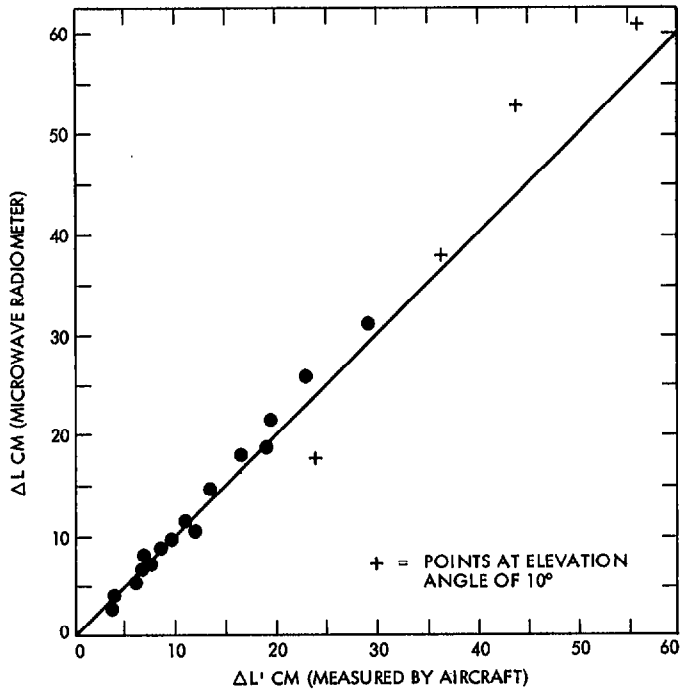

Fig. 10. Comparison of path delay as determined by an instrumented aircraft and the WVR (Pt. Mugu)

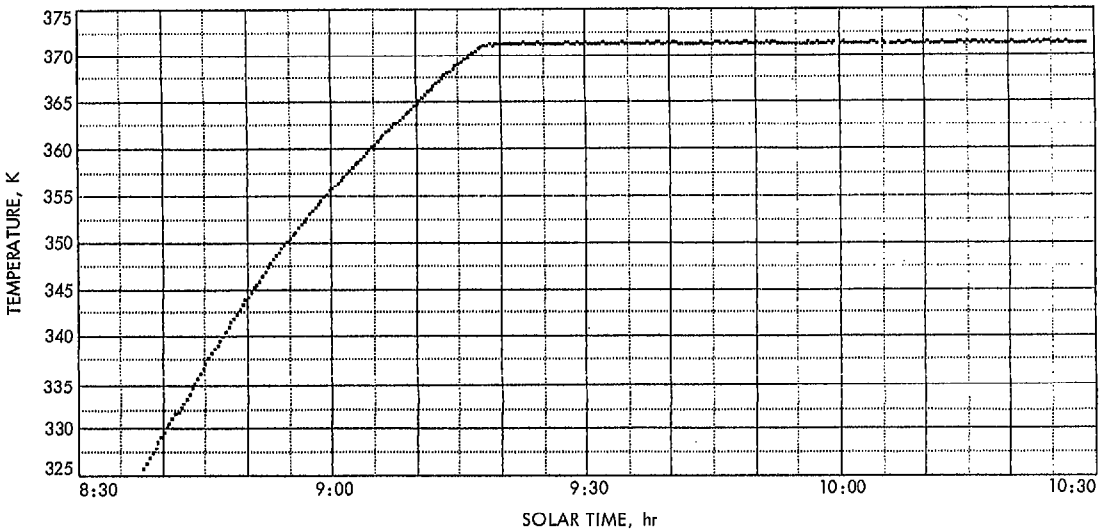

Fig. 11. Warmup characteristics of the hot load

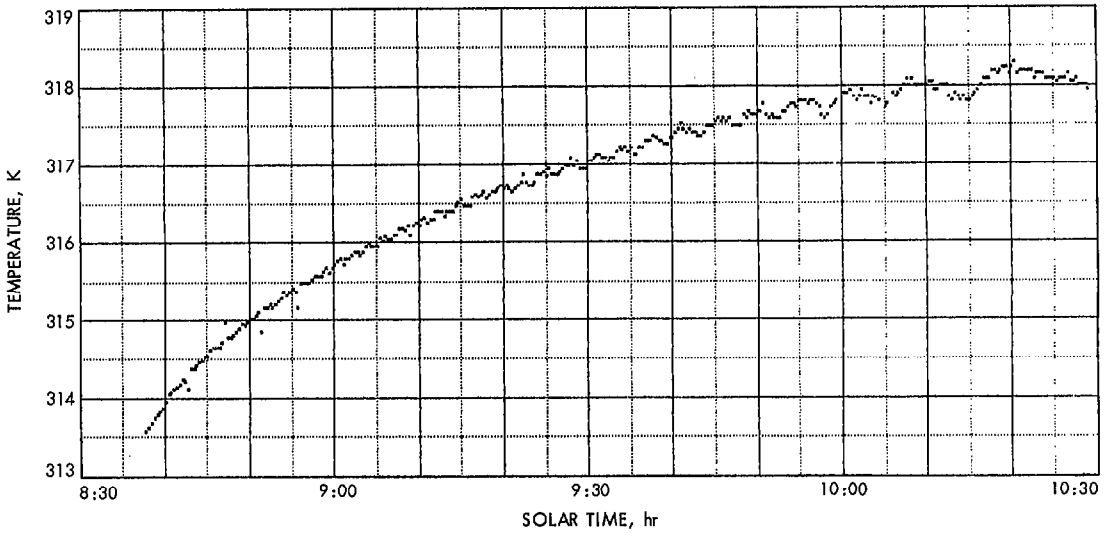

Fig. 12. Warmup characteristics of the base load

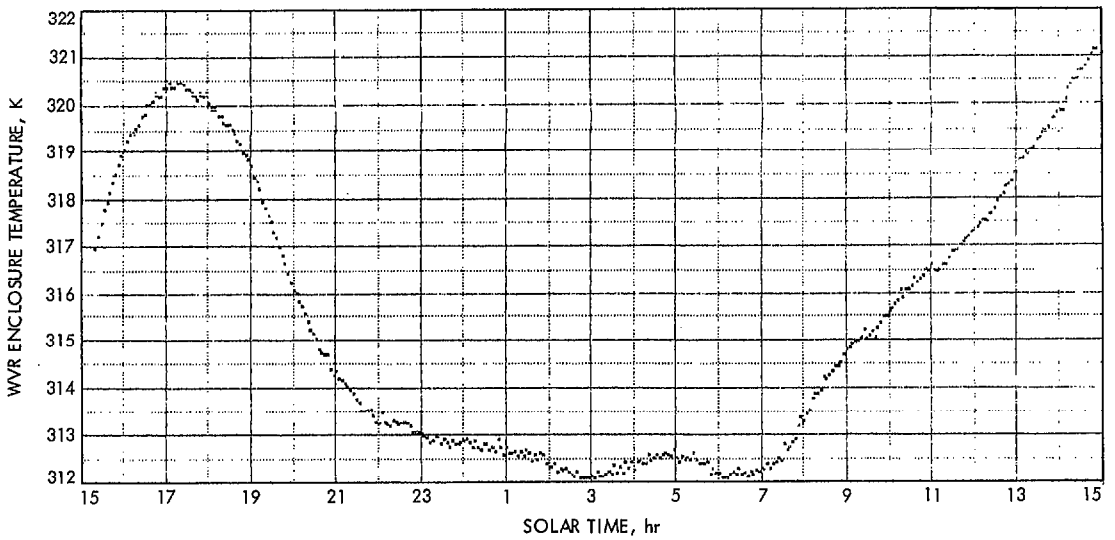

Fig. 13. Enclosure temperature vs time